ISBN: 978-3-95450-215-8 ISSN: 2226-0366 doi:10.18429/JACoW-LINAC2022-THPOJO26

CONCEPTUAL DESIGN OF THE PERLE INJECTOR

B. Hounsell* † [1,2], M. Klein, C.P. Welsch[1], University of Liverpool, Liverpool, United Kingdom
W. Kaabi, Université Paris-Saclay, CNRS/IN2P3, IJCLab, 91405 Orsay, France
B.L. Militsyn[1], STFC, Sci-Tech Daresbury, United Kingdom
[1]also at Cockcroft Institute, Warrington, United Kingdom
[2]also at Université Paris-Saclay, CNRS/IN2P3, IJCLab, 91405 Orsay, France

Abstract

Energy Recovery Linacs such as PERLE require high average current high brightness beams. This sets particular requirements on the kind of injectors that they can use as the injectors must be capable of producing bunches at MHz repetition rates, compressing the bunches to the specified value and transporting those bunches while they are still in the space charge dominated regime into the main ERL all while keeping the emittance low. In particular, PERLE will require a 20 mA beam consisting of 500 pC bunches with a repetition rate of 40 MHz. These bunches will be required to have rms lengths of 3 mm, a total beam energy of 7 MeV, appropriate Twiss parameters to match them to the main loop and transverse emittances of < 6 mm·mrad. In this paper, a DC gun based injector capable of meeting this specification will be presented with beam dynamics simulation showing the behaviour of the beam from the photocathode to the exit of the first main linac pass. The beam dynamics challenges will be discussed in terms of both the transverse emittance growth and the sources of non-linearity in the longitudinal phase space.

INJECTOR DESIGN AND SPECIFICATION

PERLE (Powerful Energy Recovery Linac for Experiements) is a proposed three turn energy recovery linac (ERL) [1, 2]. The injector is the part of the machine were the electrons are generated and the initial beam manipulations are performed before the beam enters the main ERL loop. The design of the injector is important because it sets the lower bound on the achievable beam quality. The design needs to deliver bunches at MHz repetition rates, while preserving the beam quality from the cathode, compressing the bunches to the required length, matching the Twiss parameters of the bunch to the main ERL loop and physically transporting the beam into the main ERL. A number of different injector schemes were investigated before a baseline was chosen. The layout of the baseline scheme can be seen in Fig. 1.

The injector uses a 350 kV DC electron gun. PERLE will use the ALICE electron gun [3] with planned upgrades incorporated [4]. The shape of the electrode geometry was re-optimised for PERLE [5]. After the electron gun the beam is focused and emittance compensated [6] by a pair of solenoids. A buncher cavity to compress the bunch is installed between them. There is then an SRF booster linac

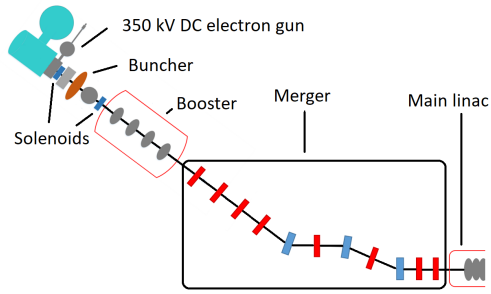

Figure 1: The layout of the PERLE injector. In the merger section quadrupoles are shown in red and dipoles in blue.

with four independently controllable single cell cavities which accelerates the beam to the injection energy of 7 MeV. The beam is then transported and matched into the main ERL loop by the merger. The merger presented here is a three dipole design which is an established design used and proposed by a number of ERL projects [7–10] . The example presented here uses four quadrupoles before the dipoles to match the beam, the quadrupoles between the dipoles to make the beamline achromatic (assuming no space charge) and two quadrupoles after the dipoles for the final matching. Only two quadrupoles are used after the dipoles due to the limited space between the final dipole and main linac.

The injector was optimised in three steps. First the electron gun electrode geometry was optimised [5] based on the beam dynamics performance using POISSON [11] to model the electrostatics, ASTRA [12] to model the beam dynamics and the many objective optimisation algorithm NSGAIII [13] as the optimisation algorithm. The injector beamline from the cathode to the exit of the booster was optimised using OPAL [14] to model the beam dynamics and again using NSGAIII as the optimisation algorithm. Then finally the merger from the exit of the booster to the exit of the first main linac pass was optimised. The matrix code Optim [15] was used to generate initial guesses for the magnet settings then the beam dynamics code OPAL and the optimisation algorithm NSGAII [14] were used for the final optimisation of the merger. At the end of this multistep optimisation procedure a solution was selected. The performance of that solution relative to the specification can be seen in Table 1.

The emittance values are within the specification. The final bunch length and Twiss parameters still require some fine tuning. The remainder of this paper will be a discussion of the beam dynamics of this chosen solution focusing on

* ben.hounsell@stfc.ac.uk
† Now at STFC, Sci-Tech Daresbury, United Kingdom

ISBN: 978-3-95450-215-8 ISSN: 2226-0366 doi:10.18429/JACoW-LINAC2022-THPOJO26

Table 1: The achieved parameters of the chosen baseline injector and the specified value both at the exit of the first main linac pass.

Parameter	Achieved	Specification
x emittance [mm·mrad]	5.0	< 6
y emittance [mm·mrad]	2.7	< 6
Bunch length [mm]	3.2	3
Beta x [m]	6.1	8.6
Alpha x	-0.48	-0.66
Beta y [m]	5.1	8.6
Alpha y	-0.17	-0.66

the emittance growth mechanisms and the formation of the longitudinal phase space.

BEAM SIZE AND BUNCH DISTRIBUTION

The evolution in beam size both transversely and longitudinally can be seen in Fig. 2. The transverse beam sizes are maintained below a target value of 6 mm rms to ensure the beam can fit through all the apertures. The quadrupoles make the beam sizes asymmetric which can clearly be seen and can be adjusted to match the Twiss parameters.

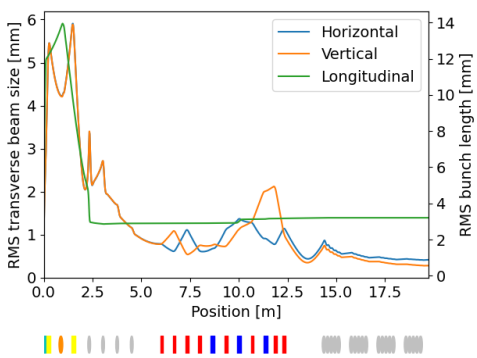

Figure 2: The rms transverse beam sizes and bunch length along the injector beamline. The location of beamline elements is shown below the plot. The electron gun is indicated in cyan, the solenoids in yellow, the buncher cavity as an orange ellipse, SRF cavities by grey ellipses, quadrupoles are shown in red and dipoles in blue.

The bunch length is initially long due to the long laser pulse on the cathode which is used to reduce the space charge forces in the gun. The bunch then expands to the position of the buncher cavity the ballistic compression begins. This ballistic bunching is the main form of compression in the injector however there is additional velocity bunching in the first cell of the booster linac. The interaction of the longitudinal dispersion of the merger and the space charge forces causes some undesirable debunching.

The charge density distribution of the bunch in both the horizontal and vertical planes of the bunch at the exit of first main linac pass can be seen in Fig. 3. There is a high density

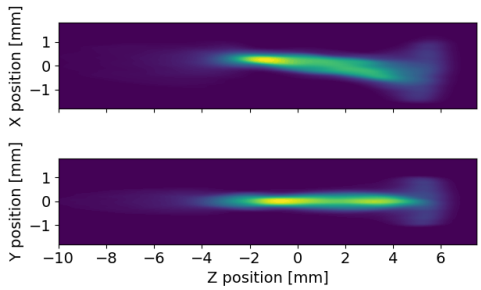

Figure 3: The charge density distribution of the bunch in the horizontal and vertical planes at the exit of the main linac.

bunch core as well as a more diffuse head and tail. The tail of the bunch forms during the ballistic bunching process due to the non-linear relationship between particle energy and particle velocity. In the horizontal plane a tilt can be seen due to residual dispersion at the end of the merger. This is a consequence of the space charge forces changing the energy of the particles, and hence how they are bent by the dipoles, as they move through the merger leading to an error in the cancellation of the dispersion.

TRANSVERSE EMITTANCE

The evolution of the transverse emittances in the injector can be seen in Fig. 4. In this figure initial emittance growth can be seen which is then compensated in the booster linac. In the merger the beam becomes axially asymmetric so the emittance evolution is asymmetric. In the horizontal plane the emittance increases significantly at the first dipole when dispersion is introduced into the beam. It then decreases significantly after the final dipole as the majority of the dispersion is cancelled. In the vertical plane the emittance grows slightly again before emittance compensating.

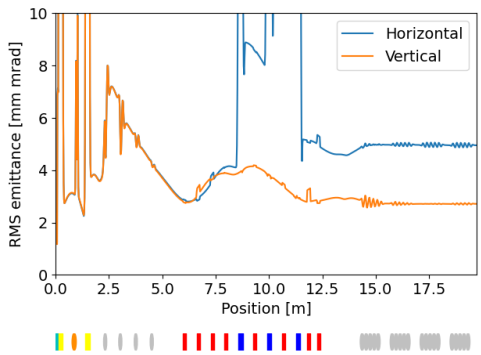

Figure 4: The rms transverse emittance along the injector beamline. The location of beamline elements in shown below the plot in the same way as in Fig. 2.

Examining the transverse phase space distributions at the end of the main linac can allow us to determine which mechanisms are responsible for the emittance growth in the

ISBN: 978-3-95450-215-8 ISSN: 2226-0366 doi:10.18429/JACoW-LINAC2022-THPOJO26

injector. The phase space distributions can be seen in Fig. 5. In both planes there are non-linearities in the phase space distributions which indicate slice emittance growth. These non-linearities can originate with non-linear space charge forces or from aberrations in the elements of the injector. It can also be seen that all of the slices are relatively well aligned rotationally with the exception of the front slice. This indicates reasonably good, but not perfect, emittance compensation. In the horizontal phase space there are also translational offsets between the slices which is indicative of residual dispersion. As discussed earlier the space charge forces in the bunch cause this residual dispersion.

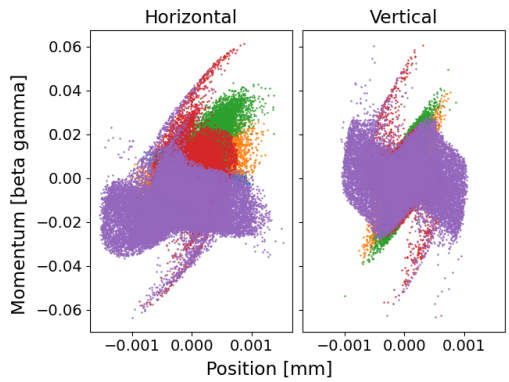

Figure 5: The transverse phase space distributions at the end of the main linac. The bunch has been sliced longitudinally into five slices, indicated by colour, so the slice rotations and translations can be clearly seen. The slices by colour from front to back are purple, red, green, orange and blue.

It may be possible to mitigate some of the emittance growth mechanisms discussed above. Modifying the electron distribution by shaping the photoinjector laser pulse could reduce the non-linear space charge forces and hence the slice emittance growth [16]. The emittance growth due to the residual dispersion could be reduced by matching the longitudinal space charge (LSC) kick at the exit of the dispersive region with the Twiss parameters of the bunch at that point [17]. The kick at that point determines the orientation of the axis in phase space along which the slices are offset. If the beam ellipse has the same orientation at that point the emittance due to the LSC kick will be minimized. In the case of the injector presented here this matching can't be achieved as there are only two quadrupoles between the final merger dipole and the main linac so there aren't enough adjustable elements to achieve the match while matching the vertical Twiss parameters to the main ERL loop. If the available space here was increased two quadrupoles could be added to give sufficient adjustable elements.

LONGITUDINAL PHASE SPACE

In addition to the transverse emittances of the beam the longitudinal phase space distribution is also important. Ideally it should be as linear as possible to minimise the energy spread at the interaction point. The longitudinal phase space of the bunch just prior to entering the main linac can be seen in Fig. 6. The motivation for looking at the longitudinal phase space at this point is so that the phase space non-linearities which develop specifically in the injector can be seen without the effect of the main linac. In the plot it can be seen that there has not being significant longitudinal slice mixing. This is the desired behaviour as slice mixing is incompatible with the emittance compensation technique used in the injector [6].

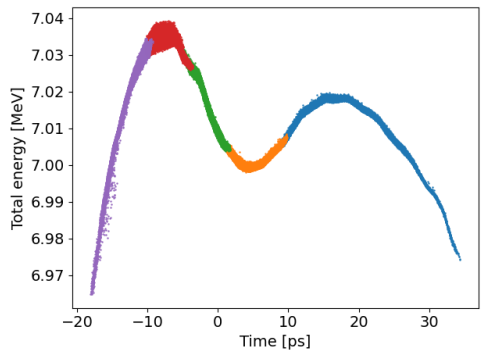

Figure 6: The longitudinal phase space distribution just prior to entering the main linac. The particle colour indicates initial longitudinal slice.

An "M" shaped non-linearity can be seen in the longitudinal phase space distribution. This is due to the combination of a number of different non-linearities. The central dip originates from the ballistic bunching process. When the bunch is longitudinally focused down to a waist the space charge forces push outwards reversing the bunching. As the charge distribution is asymmetric, due to the diffuse tail discussed earlier, the longitudinal space charge forces are also asymmetric. As a result the head of the bunch starts debunching before the tail. At this point during the bunching the longitudinal phase distribution is a "V" shape. The bunch is then accelerated by the booster cavity. The booster introduces a second order RF non-linearity which is the outer "wings" of the "M" shape. The asymmetry in the height of the two peaks of the "M" shape develops in the merger due to space charge induced chirp that develops at the front of the bunch where the charge density is highest.

CONCLUSION

In this paper a conceptual design of the PERLE injector which meets the specification has been presented. The source of emittance growth in the transverse phase spaces were discussed. The origin of the "M" shape longitudinal phase space due to the ballistic bunching process, booster linac RF distortion and a space charge induced chirp developing in the merger was also discussed. The use of laser pulse shaping and the addition of quadrupoles to allow for LSC kick matching were presented as possible future directions to reduce the emittance. Following this conceptual design the next will be the technical design.

ISBN: 978-3-95450-215-8 ISSN: 2226-0366 doi:10.18429/JACoW-LINAC2022-THPOJO26

REFERENCES

[1] W. Kaabi *et al.*, "PERLE: A High Power Energy Recovery Facility", in *Proc. 10th Int. Particle Accelerator Conf. (IPAC'19)*, Melbourne, Australia, May 2019, pp. 1396–1399. doi:10.18429/JACoW-IPAC2019-TUPGW008

[2] D Angal-Kalinin *et al.*, "Neutrino production states in oscillation phenomena—are they pure or mixed", *J. Phys. G: Nucl. Part. Phys.*, vol. 45, p. 065003, 2018. doi:10.1088/0954-3899/35/6/065003

[3] F. Jackson *et al.*, "The Status of the ALICE Accelerator R&D Facility at STFC Daresbury Laboratory", in *Proc. 2nd Int. Particle Accelerator Conf. (IPAC'11)*, San Sebastian, Spain, Sep. 2011, paper TUODA03, pp. 934–936.

[4] B. L. Militsyn *et al.*, "Design of an Upgrade to the ALICE Photocathode Electron Gun", in *Proc. 11th European Particle Accelerator Conf. (EPAC'08)*, Genoa, Italy, Jun. 2008, paper MOPC073, pp. 235–237.

[5] B. Hounsell *et al.*, "Re-optimization of the ALICE gun upgrade design for 500 pC bunch charge requirements for PERLE ", in Proc. 10th Int. Particle Accelerator Conf. (IPAC'19), Melbourne, Australia, May 2019, paper TUPTS066. doi:10.18429/JACoW-IPAC2019-TUPTS066

[6] B. E. Carlsten, "New photoelectric injector design for the Los Alamos National Laboratory XUV FEL accelerator", *Nucl. Instrum. Methods Phys. Res., Sec. A*, Vol 285, Issues 1–2, 1989, Pages 313-319, doi:10.1016/0168-9002(89)90472-5

[7] C. Hernandez-Garcia *et al*, "Performance and Modeling of the JLab IR FEL Upgrade Injector", in Proc. *26th International Free Electron Laser Conference and 11th FEL User Workshop*, 2004, Trieste, Italy, 29 Aug - 3 Sep 2004, paper TUPOS61.

[8] B, Kuske *et al*, "The injector layout of BERLinPro", in *Proc. 4th Int. Particle Accelerator Conf.(IPAC'13)*,, Shanghai, China, May 2013, paper MOPFI004, pp. 288–290.

[9] G, Hoffstaetter *et al*, "CBETA Design Report", 2017

[10] JG, Hwang *et al*"Effects of space charge in a compact superconducting energy recovery linac with a low energy"in *Nucl. Instrum. Methods Phys. Res., Sec. A*, Volume 684, 2012, Pages 18-26,

[11] *Poisson Superfish* [Online], Avaliable: https://laacg.lanl.gov/laacg/services/download_sf.phtml

[12] K. Floettmann (1997), *ASTRA: A Space Charge Tracking Algorithm* [Online], Avaliable: http://www.desy.de/~mpyflo/

[13] K. Deb and H. Jain, "An Evolutionary Many-Objective Optimization Algorithm Using Reference-Point-Based Nondominated Sorting Approach, Part I: Solving Problems With Box Constraints", in *IEEE Transactions on Evolutionary Computation*, vol. 18, no. 4, pp. 577-601, Aug. 2014. doi:10.1109/TEVC.2013.2281535

[14] A. Adelmann *et al*, "OPAL a Versatile Tool for Charged Particle Accelerator Simulations", [arXiv:1905.06654 [physics.acc-ph]].

[15] "Optimx: A Program For Accelerator Optics", [online] Available at: https://home.fnal.gov/$\sim$ostiguy/OptiM [Accessed 11 December 2020]

[16] F. Zhou *et al*, "Experimental Studies with Spatial Gaussian-cut Laser for the LCLS Photocathode Gun"in textitProceedings of FEL'11, Shanghai, China, Aug. 2011, paper WEPA06, pp. 341–344.

[17] V. Litvinenko *et al*, "Merger designs for ERLs"in *Nucl. Instrum. Methods Phys. Res., Sec. A*, Vol 557, Issue 1, 2006, Pages 165-175.